Mathematical and Computational Modeling of Diffusion-Based Transport from Differing Designs of Drug-Containing Sutures

S. N. Jorgensen[1], J. R. Sanders[1]
1. Department of Chemical Engineering, Tennessee Technological University, Cookeville, TN, USA

Introduction

Components of the dermal wound healing process must work in a well-orchestrated, intertwined chain of events to accomplish successful closure and healing of the dermal wound [1], [2]. Typically, the wound healing process is explained by four main phases: hemostasis, inflammation, proliferation, and remodeling [1]—[4]. However, some wounds are too deep or complexly-shaped to simply proceed through the phases of dermal wound healing without a facilitated closure method, including but not limited to sutures, staples, or adhesives. While studies that examine the prevalence and cost of non-healing wounds in the United States are lacking, estimates predict a prevalence rate between 3 and 6 million cases per year and total cost exceeding $3 billion per year in the US [1], [5]. According to studies completed in 2013, 2.7% of patients that received emergency care required suturing procedures [6]. According to Bayat *et al.*, suturing procedures due to trauma or elective operations could result in up to 11 million keloid scars in the developed world [7].

Arno *et al.* state that it "is more efficient to prevent excessive scars than to treat them" [8]. Researchers have indicated that prevention of such excessive scarring that characterizes keloid scars can occur with control of the wound healing process; specifically, achieving good hemostasis [9], [10] and controlling the rates of collagen fiber synthesis and deposition [11], [12] during the wound healing process reduces the potential for excessive scarring, like keloids, to result. Uitto *et al.* further state "there is a distinct need for further development of novel approaches to control collagen accumulation in patients with connective tissue abnormalities" that have been shown to lead to keloid scars [12].

Many therapeutic formulations have been investigated for their healing properties with the goal to reduce or eliminate scarring, especially with respect to keloid scars that result from abnormal healing. The standard treatment for keloid scars is intralesional delivery of corticosteroids [8]—[10], [13], [14], however, some success in reduction of keloid scarring has been shown with other injectable therapies such as 5 fluorouracil (5-FU) [14]—[20], and interferon-γ (IFN-γ) [13], [21]—[23]. Scar creams and topical agents have been suggested for use to reduce scar appearance [24]—[26]. Applications and administrations of growth factors, such as platelet-derived growth factor (PDGF) and transforming growth factor-β (TGFβ), have been indicated to initiate certain actions of the healing process, promoting healing and potentially reducing complications with scarring [27]—[30].

For wounds that require facilitated closure procedures such as suturing, infection poses a resistance to a normal wound healing pattern, and infected wounds often result in abnormal or impaired healing [31]. In fact, the presence of sutures in a tissue has been said to increase that tissue's susceptibility to infection [32], [33], and certain suture types increase the risk of potentiating infection [32]—[34]. Therefore, to diminish these high rates of pathological healing conditions and large numbers of resultant scars, targeted drug delivery in the wound offers the potential to provide local therapeutics to the site of wound healing in a time- and spatially-dependent manner in an attempt to assist the process of wound healing in progression through the phases of healing.

Despite the indication for the delivery of medications to sites of dermal injury requiring facilitated closure, there is little validation of the concentration profiles that might result from using sutures to deliver medication to a wound that might ensure that wound healing proceeds optimally. Experimentation alone that might yield this information would be costly and require extensive amounts of time, making mathematical modeling and simulation an attractive complement for initial explorations to study the effects of drug delivery to a dermal wound from a permeable and/or drug-coated suture. In this work, the predicted concentration profiles of a hypothetical medication within a dermal wound following diffusion from various drug-loaded suture designs is determined with COMSOL Multiphysics (Version 5.0, Burlington, MA) simulation. For the most simplistic design considered, analytical modeling efforts were used in parallel to COMSOL modeling

to justify the physics and associated conditions of the design.

Theory / Experimental Set-up

COMSOL Simulation: A Suture Design that Releases Drug through a Fixed Concentration Boundary (Case 1)

For most mathematical approaches, it is beneficial to begin mathematical modeling with the most simplistic case. Here, the most simplistic case considers a suture design that releases a drug-simulant through a fixed concentration boundary between the suture and the wound domain. To achieve this release through a fixed concentration boundary, a suture is envisioned as having two domains (Figure 1 and Figure 2). The first domain of the suture (labeled #1 in Figure 1 and Figure 2) represents an area within which the drug would be pre-loaded prior to suture placement. The second domain of the suture (labeled #2 in Figure 1 and 2) is envisioned to accommodate accumulated drug released from domain 1 before the drug is released into the wound domain. Domain 1 would in effect serve as a source of drug. The staggered release rate may be facilitated by the suture design, where the design might incorporate a porous membrane to control the rates at which the drug diffuses from the first domain into the second domain as well as from the second domain into the wound domain. This could potentially be achieved by having an interface between domains 1 and 2 that is much less restrictive than the interface between domain 2 and the wound. Additionally, controlling the relative volumes of domain 1 to domain 2 would allow further control of staggered drug release. Domain 1 might be designed to have a larger volume than domain 2. These relative sizes of domain 1 to domain 2 would ensure the source of the drug would not deplete so quickly that the concentration of the drug in domain 2 varied considerably over a desired time interval. The relatively small volume of domain 2 in addition to the high permeability of the interior porous membrane would allow the drug to accumulate in domain 2 such that a relatively constant (or fixed) concentration is also established in this domain. Once the suture is placed, the relatively smaller permeability of the exterior porous membrane (separating domain 2 and the wound domain) combined with the other design features discussed above would allow drug release at a known, fixed concentration. This conceptual design and related justification allows for an analytical solution of the transient concentration profile in a wound to be used along with a COMSOL simulation (and eventually experimentation) to maximize the information learned about each suture design.

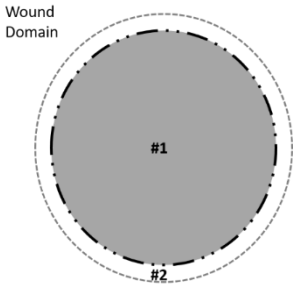

Figure 1 Cross-sectional view of the conceptual suture design indicating the interior drug-loading domain (#1) and the outer transport domain (#2) of a suture after it is placed in the wound domain.

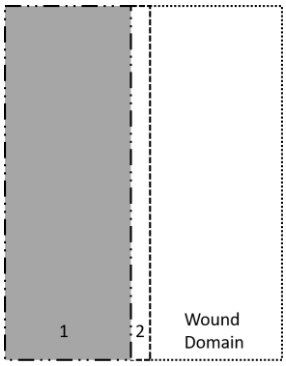

Figure 2 Two-dimensional (2-D), axisymmetric, rectangular view of the conceptual suture design indicating the interior drug-loaded domain (#1) and the outer transport domain (#2) of a suture after it is placed in the wound domain.

To test such a design in COMSOL Multiphysics (Version 5.0), a singular 2-D, rectangular area with a width of 0.42 mm and a height of 3 mm was used to depict a wound domain outside of a placed suture. In other words, the left-most boundary of the rectangular wound domain correlated to the right-most edge of the transport domain (#2) (Figure 3). By viewing the simulation design in Case 1 as a single rectangle, domains 1 and 2 in Figures 1 and 2 were eliminated from the simulation with only the fixed concentration of the drug along the boundary of domain 2 and the wound domain being considered by the modeling parameters. A no-flux boundary condition was applied to the right-most boundary of the wound domain as the distance from the suture to the edge of this wound domain was assumed to be far enough away that the amount of drug simulant reaching this point was essentially zero, thus establishing either a zero concentration or no-flux boundary condition there. The top and bottom boundaries of the wound domain also utilized no-flux

boundary conditions, as the drug simulant is assumed to be diffusing only through the defined wound domain. Details of the parameters used in the COMSOL model are indicated in Table 1 in the Appendix.

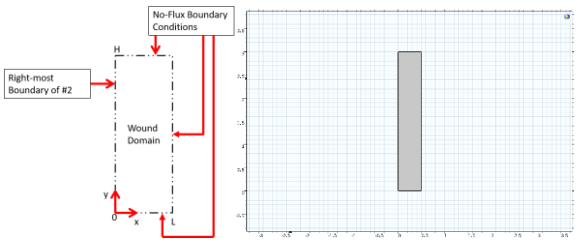

Figure 3 2-D simulation domain of the wound area of Case 1 (COMSOL domain shown to the right).

Governing Equation

An analytical model was also developed to complement the results of the simulation for the most simplistic mathematical case of a drug simulant diffusing from the suture with a fixed concentration boundary. For the domain of Figure 3, the species continuity equation was applied and solved subject to boundary and initial conditions.

$$\frac{\partial C_A}{\partial t} = D_A\left[\frac{\partial^2 C_A}{\partial x^2} + \frac{\partial^2 C_A}{\partial y^2}\right]$$

COMSOL Simulation: A Drug-Coated Solid Suture (Case 2)

Drug-coated sutures are already being investigated for their drug-release properties [35]—[37]. A simulation has therefore been developed to represent the drug release properties and concentration profiles that would result in a wound domain with consideration of this suture design. For these purposes, this drug-coated solid suture design was created in COMSOL Multiphysics (Version 5.0) using a 2-D domain representative of the exterior of a drug-coated solid suture situated inside an encompassing wounded dermal tissue domain. In other words, the interior of the suture is not included in the COMSOL simulation for this suture design. Instead, the assumption was made that the drug would not diffuse into the interior of the suture but only into the wound domain. This was modeled with no-flux boundary conditions at the left-most boundary, as described below. Visually, the domain constructed consisted of two rectangular areas; the first represented the drug-coated portion of a suture with a width of 0.08 mm and a height of 3 mm, and the second represented the wounded dermal tissue again with a width of 0.42 mm and a height of 3 mm (Figure 4).

The model incorporates equations reflecting those for species mass "transport in porous media" (an available "physics" in COMSOL) through the drug-coated portion of the suture as well as in the wound domain as the dermal tissue is a porous media. However, for the wound domain, the porosity was set to equal a value of one as the porosity of dermal tissue is, for modeling purposes, considered variable between zero and one. This range represents the lower and upper limits in COMSOL, with a value of one corresponding to a highly porous space equivalent to the behavior of the COMSOL "transport of diluted species" physics in the defined wound domain. Thus, even though the "transport in porous media" physics module is used for the wound domain in Case 2, the fact that we set the porosity equal to one allows direct comparison to Case 1, as the "transport of diluted species" physics was used within that wound domain.

Initially, the concentration of the drug simulant was specified to be an arbitrary 1,000 mol/m^3 in the porous domain representing the drug coating and 0 mol/m^3 in the wound domain. The model was specified to have no-flux boundaries surrounding the exterior of the domains. (In other words, the top and bottom boundaries of domains 1 and 2 in Figure 4, as well as the left- and right-most boundaries of domains 1 and 2, respectively, require a no-flux boundary condition.) More details regarding the parameters of the model are included in Table 1.

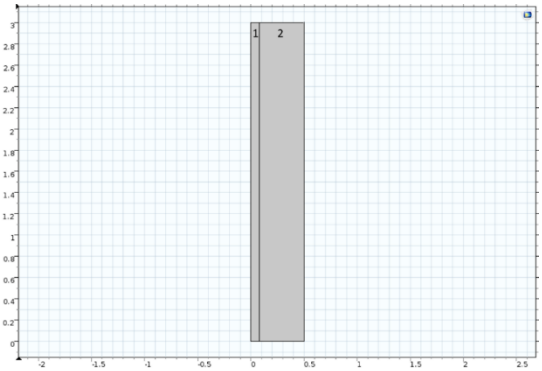

Figure 4 2-D domain constructed in COMSOL to represent Case 2. From left to right, (1) represents the coated portion of a drug-coated suture and (2) represents the wounded dermal tissue.

COMSOL Simulation: A Drug-Loaded, Hollow Suture with Porous Wall (Case 3)

Similar to the suture design imagined for Case 1, a suture design has also been investigated that allows a

drug to be loaded into the interior of the suture, diffuse through a porous wall of the suture, and release drug via diffusion into a wound. While the design of the suture correlates somewhat with Case 1, the COMSOL domain was modified to include the three domains rather than considering only the wound domain as in Case 1. In effect, this allowed us to not have to assume an infinite source domain. COMSOL was used to construct 2-D, axisymmetric simulation domains. These domains were representative of a drug-loaded, porous suture situated inside an encompassing wounded dermal tissue domain. Visually, the domain constructed consisted of three rectangular areas as stated; the first represented the interior of the drug-loaded suture with a width of 0.2 mm, the second represented the thickness of the porous suture wall with a width of 0.08 mm, and the third represented the wounded dermal tissue similar to the other cases with a width of 0.42 mm (Figure 5). All domains had a height of 3 mm. The model incorporated equations reflecting the transport of dilute species in both the interior of the drug-loaded suture and wound domains and equations for species mass transport in porous media through the wall of the suture. Such might be the case physically assuming that the initial concentration of the drug simulant within the interior suture domain is 1,000 mol/m^3 and that the initial concentration of the drug simulant in the porous wall of the suture as well as the wound domain is 0 mol/m^3. The interior suture and wound domains are considered a non-porous material (porosity of 1), and as before, there are no-flux boundaries surrounding the exterior of the domains (in other words, the top and bottom boundaries of domains 1, 2, and 3, as well as the right-most boundary of domain 3 require a no-flux boundary condition). The boundary at r = 0 requires a symmetry condition as the 2-D domain presented in Figure 5 represents a cylindrical geometry physically. These parameters, and others, are summarized in Table 1 along with a comparison between the three COMSOL models.

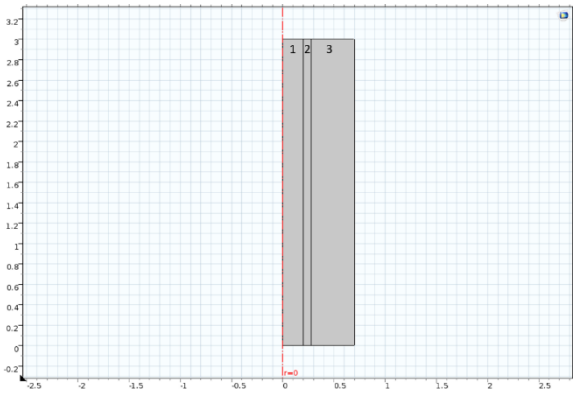

Figure 5 2-D, axisymmetric domain constructed in COMSOL to represent Case 3. From left to right, (1) represents the center of the drug-loaded suture, (2) represents the thickness of the porous wall of the suture, and (3) represents the wounded dermal tissue.

Simulation Results

Case 1: A Suture Design that Releases Drug through a Fixed Concentration Boundary

A time-dependent study (Figure 6) showed, as expected, that the drug simulant was highly concentrated at the boundary correlating to the suture edge, and as time progressed the drug simulant diffused from the suture through the wounded dermal tissue domain. For each of the three time points plotted, the x-axis corresponds to the distance into the wound domain while the y-axis provides the concentration. At a "long time" correlating to about an hour after the initial time, the COMSOL simulation shows the drug simulant has dispersed in a manner to achieve an almost even distribution of the drug simulant through the domain. Figure 7 shows the concentration profile that develops over time at a given position (x = 0.24459 mm) within the wounded dermal tissue domain. Specifically, a line was defined such that COMSOL would examine the concentration profile along the line only. For this purpose, the line was plotted vertically from (0.24459, 0) to (0.24459, 3) (where the points of the lines included herein have units of mm), producing Figure 7 which indicates that as time passes, the concentration of the drug simulant at this position increases in the wounded dermal tissue domain until it reaches the concentration of the boundary.

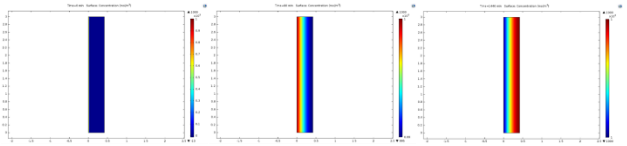

Figure 6 The time-dependent concentration of a drug simulant through the wounded tissue domain of Case 1 at a) 0 minutes, b) 60 minutes, and c) 1,440 minutes.

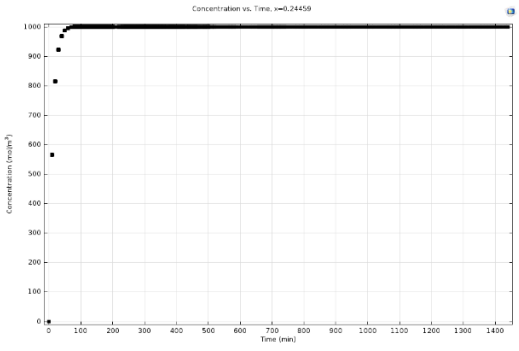

Figure 7 The concentration profile that develops over time along a specified cut-line within the wound domain of Case 1 (x = 0.24459 mm).

To show how the concentration profile of the drug simulant changes with time over the entire wound domain, a cut-line was defined horizontally (in the x-direction), specifically from the position (0, 0.2) to the position (0.5, 0.2), to produce Figure 8. At t = 0 minutes, per the prescribed initial and boundary conditions, Figure 8 shows that the concentration of the drug simulant exhibits a sharp difference at the interface of the fixed concentration boundary with the wound domain. The uneven curvature that occurs from an x-coordinate of about 0.025 mm to 0.07 mm is most likely due to irregularities of the meshing used by COMSOL for this simulation at those positions. Though all COMSOL simulations were performed with an "extremely fine" meshing setting, irregularities in the results such as shown in Figure 8 were sometimes seen. This correlates with the immediate diffusion of the drug simulant along the concentration gradient that develops from the fixed concentration along the boundary (with an arbitrary initial value of 1,000 mol/m^3) to just inside the boundary of the wound domain where the initial concentration of drug simulant is equal to 0 mol/m^3. The sharp slope of the profile at a time of 0 minutes indicates that the rate of diffusion is initially relatively fast. As the concentration of the drug increases in the wound domain, indicating the drug is accumulating in the wounded dermal tissue (as it is not being consumed due to the assumption that no reaction is occurring in the bulk of the wound domain nor is it assumed to leave through the vasculature), the slope of the profile drastically decreases to a nearly-horizontal line at a time of approximately one hour. This represents a slower rate of diffusion. As time increases, this effect continues until eventually the concentration is reflected by a straight line, indicating there is no net transfer of species mass within the wound domain and the concentration of the drug is uniform throughout the wound domain and the same as that in the suture.

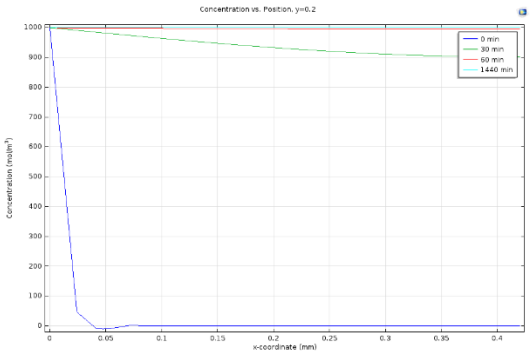

Figure 8 The concentration profile that develops along a specified cut-line within the wound domain of Case 1 (y = 0.2 mm).

As seen in this figure, the transient concentration profile obtained by the complementary analytical solution (when the series solution coefficient, m, is varied from 1 to 3) at the same position as the solution obtained by COMSOL (x = 0.24459 mm) follows the trend of the one obtained with the COMSOL simulation.

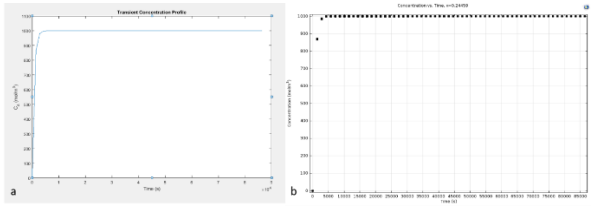

Figure 9 The results of the analytical and simulation models of the transient concentration profile for Case 1. **a)** The analytical solution of the transient concentration profile of the drug simulant within the wound domain for Case 1. x=0.24459 mm, t varied from 0 seconds to 86,400 seconds in increments of 1,440 seconds. **b)** The simulation solution by COMSOL of the transient concentration profile of the drug simulant within the wound domain for Case 1. x=0.24459 mm, t varied from 0 seconds to 86,400 seconds in increments of 1,440 seconds.

Case 2: A Drug-Coated Solid Suture

When examining a drug-coated solid suture in which the drug layer is assumed to have a porosity of 0.3 (max = 1.0), a time-dependent study of the domain of Figure 4 showed that at a time of 0 minutes, the drug simulant was only found (as expected) in the drug coating where it was defined to have an initial concentration of 1,000 mol/m^3 (*i.e.*, domain 1 as shown in Figure 4). As time increased and the drug simulant was diffusing through the simulation domains, the concentration of the drug simulant decreased in the drug-coated portion of the suture and increased in the wound domain as expected. After about 12 hours, the drug simulant neared a uniform distribution, and after 24 hours, it reached a concentration of 54.1 mol/m^3 throughout the entire simulation domain (Figure 10). The effects of porosity were examined for this domain as well by exploring the effects of an assumed porosity of the drug coating of either 0.3, 0.6, and 0.9 (Figure 11). Figure 11 shows that the final concentration within the entire simulation domain for Case 2 increases with increasing porosity of the drug-coated portion of suture domain.

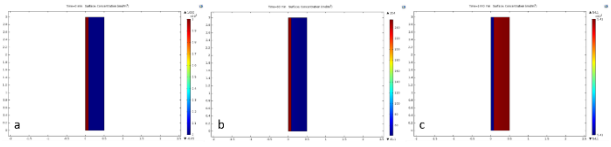

Figure 10 The time-dependent concentration of a drug simulant through the domains of Case 2 with porosity 0.3 in the drug coating at a) 0 minutes, b) 60 minutes, and c) 1,440 minutes and a porosity of 1 in the wound domain.

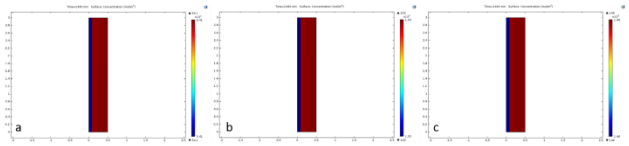

Figure 11 The effect of variation of the porosity of the drug coating on the solid suture wall on the eventual distribution of drug simulant within the domains of Case 2 for porosities a) 0.3, b) 0.6, and c) 0.9 (with a porosity of 1 in the wound domain).

As for Case 1, cut-lines were defined in COMSOL to gain understanding of the concentration profile as it changed versus time and position. For the concentration profile that developed over time in the wound domain (Figure 12), the vertical cut-line was positioned from (0.32459, 0) to (0.32459, 3), corresponding to a position 0.24459 mm into the wound domain as to be comparable to the results of Case 1. Figure 12 shows that while the diffusion from the drug-coated portion of the suture into the wound domain of Case 2 occurs quickly (reaching equilibrium within about 3 hours), it occurs more slowly relative to Case 1. The eventual uniform distribution of drug simulant through the simulation domain is shown graphically in the concentration profile plotted against x-position in the simulation domains (Figure 13).

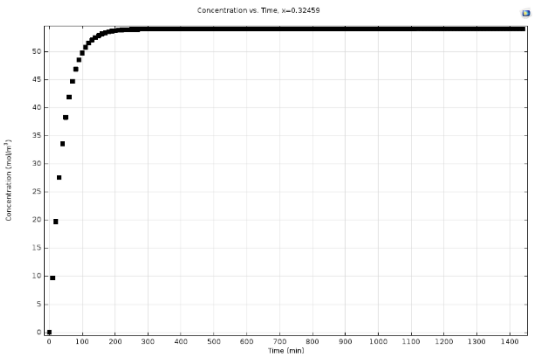

Figure 12 The concentration profile that develops along a specified cut-line within the domain for Case 2 with porosity of 0.3 in the drug coating (x = 0.32459 mm).

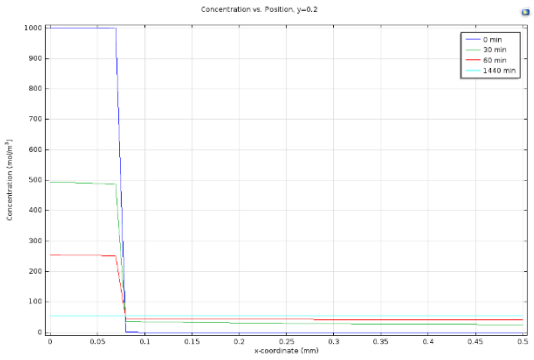

Figure 13 The concentration profile that develops along a specified cut-line within the domain for Case 2 with porosity of 0.3 in the drug coating (y = 0.2 mm) for times corresponding to 0, 60, and 1,440 minutes.

Case 3: A Drug-Loaded, Hollow Suture with Porous Wall

Once again, a time-dependent study showed, as expected, that the drug simulant was highly concentrated in the interior of the suture initially (as the initial condition dictated), and as time progressed, the drug simulant diffused through the porous wall of the suture and into the wounded dermal tissue domain. After about twelve hours, the COMSOL simulation shows the drug simulant has dispersed in a manner to achieve an almost even distribution of the drug simulant throughout the domains of Case 3. This distribution becomes even less varied after twenty-four hours, indicating that the drug simulant has obtained an almost-uniform distribution after diffusing through the domains of Case 3 for one day (Figure 14). The porosity of the suture wall was varied to gain an understanding of the effects of the suture's porosity on the transport properties of the drug simulant through the suture and tissue domain of Case 3 (Figure 15). Finally, 3-D plots were developed to envision the distribution in a more realistic representation (Figure 16).

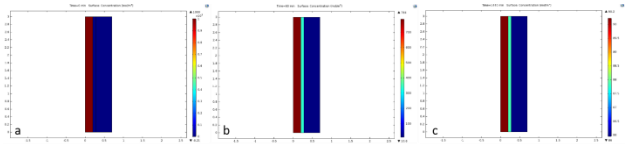

Figure 14 For a porosity of the suture wall equal to 0.3 (unitless), the figure shows the time-dependent concentration of a drug simulant throughout domain of Case 3 at a) 0 minutes, b) 60 minutes, and c) 1,440 minutes.

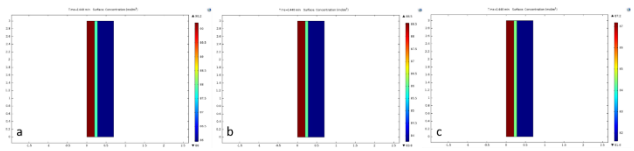

Figure 15 The effect of variation of the porosity of the suture wall on the eventual distribution of drug simulant at t = 1,440 minutes within the domain of Case 3 for porosities a) 0.3, b) 0.6, and c) 0.9 (porosity of 1 in the wound domain).

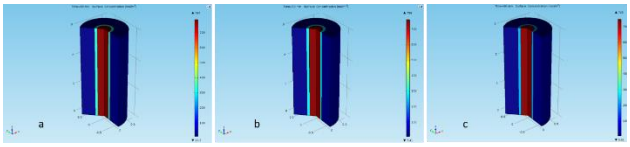

Figure 16 3-D plots of the eventual distribution at t = 1,440 minutes in the domains of Case 3 for porosities a) 0.3, b) 0.6, and c) 0.9 (porosity of 1 in the wound domain).

Again, cut-lines were developed within the wound domain to show how the concentration profile was changing with time (Figure 17) and position (Figure 18). The vertical cut-line was positioned in a manner that would correlate with the placement of the cut-line for Cases 1 and 2. Therefore, the cut-line for Case 3 was placed at 0.32459 mm as the wound domain is not defined until 0.08 mm in the COMSOL design. Figure 17 shows the concentration profile at this position for the duration of the COMSOL simulation. It indicates that initially, the concentration of drug simulant within the wound domain of Case 3 is 0 mol/m^3, and this value increases to approximately 85 mol/m^3. The slope of the increase in concentration indicates that diffusion within this domain initially occurs relatively quickly. The defined curvature of the profile in Figure 17 relative to Figures (7) and (12) indicates that the diffusion within the simulation domains for Case 3 occurs more slowly than for Cases 1 and 2.

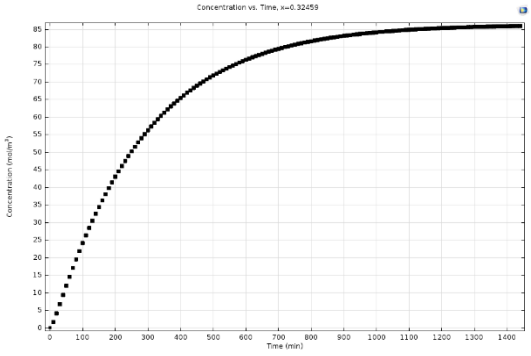

Figure 17 The concentration profile that develops along a specified cut-line within the domain of Case 3 with porosity of 0.3 (x = 0.32459 mm).

As before, a horizontal cut-line at a y-position (correlating to a z-position as the domain defined in COMSOL is a 2-D axisymmetric domain representing a cylinder) of 0.2 mm has been used to determine the concentration profile as it changes with position. Figure 18 shows this concentration profile for each domain of Case 3, specifically, the interior suture domain, the porous suture wall, and the wound domain from left to right, respectively. The profile shows that the initial concentration of the drug simulant (1,000 mol/m^3) remains constant until the boundary of the porous wall of the suture (0.2 mm) where there is an immediate decrease to a value of 0 mol/m^3, which is the specified initial value of the drug simulant within the porous suture wall and the wound domain. It makes sense, then, that the value remains at 0 mol/m^3 through the rest of these simulation domains at the initial time (0 minutes). At a time of 60 minutes, the concentration has dropped in the interior suture domain from 1,000 mol/m^3 to approximately 790 mol/m^3. Recalling that the axisymmetric rectangular domains are actually representative of a cylindrical domain, this decreased value indicates the drug is diffusing from the interior of the suture into the porous wall of the suture and finally into the wound domain. Eventually, the concentration within the entire domain (the interior suture, suture wall, and wound domains) has distributed in a more uniform manner, indicated by the profile at 1,440 minutes.

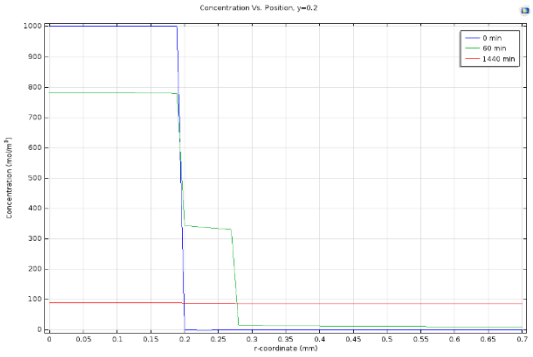

Figure 18 The concentration profile that develops along a specified cut-line within the domain of Case 3 with porosity of 0.3 (y = 0.2 mm).

Discussion

To best provide comparable results, each simulation was constructed in a consistent manner by first thoughtfully constructing a theoretical domain and then applying similar physics for each case. To further maintain comparability, the initial conditions, while applied to various parts of the domain depending on the case being modeled, had the same value for the corresponding domains in each simulation. Similarly, for Case 2 and Case 3, the flux boundaries were constructed in the same manner despite the differences between the simulations. Table 1 provided a full list of the parameters and variables used for each case.

Interestingly, the one-rectangle domain with a fixed concentration of the drug simulant at the left-most boundary of the wound domain (Case 1) showed the time to reach a uniform distribution of drug simulant throughout the wound domain is slightly longer than an hour with the provided parameters (Figures 6 and 7). Contrastingly, Case 2 and Case 3 showed that the time for the drug simulant to distribute uniformly within these simulation domains is longer than an hour (Figures 12 and 17), and the diffusion occurs more slowly in these cases relative to Case 1. The final concentration values in both Case 2 and Case 3 are far less than the initial concentration of drug simulant (1,000 mol/m^3), whereas the final concentration reached in Case 1 is consistent with the initial concentration of drug simulant. Certainly, this would change as, realistically, the source domain is sufficiently depleted of drug due to continued usage of the suture combined with actual removal of the drug from the wound domain via metabolism and/or removal via the vasculature.

As indicated by Table 1, the COMSOL models that included the study of species transport in porous media were those provided by the model representing a drug-coated solid suture (Case 2) and a drug-loaded hollow suture (Case 3). The results for these cases indicate that the porosity of the drug coating and the suture wall affects the amount of drug simulant that is delivered to the wounded dermal tissue domain. Specifically, for Case 2, as the porosity of the drug-coated portion of the suture increases from 0.3 to 0.9, the final concentration values increase for the entire simulation domain during the given time range (Figure 11) due to higher drug loading at higher porosities in the porous drug coating (Case 2) and increased ease for the drug to diffuse through the coating domain and into the wound domain (Cases 2 and 3). However, for Case 3, the higher the porosity of the wall of the suture, the lower the amount of drug simulant that is delivered to the wounded dermal tissue domain for a given amount of time (Figures 15 and 16). With a higher porosity of the porous suture wall, a larger amount of drug simulant is required to saturate the porous wall of the suture compared to a less-porous suture wall, potentially resulting in less overall delivery of the drug simulant to the wounded dermal suture domain. These differences are associated with differences in the overall amount of the drug simulant being modeled by either case. Specifically, in Case 2, the initial mass of drug simulant is loaded into the drug coating on the solid suture surface. With an area of the drug-coated solid suture portion of the domain of 0.00024 m^2, the amount of drug simulant per unit area and unit length is 0.24 mol. However, in Case 3, the initial concentration is loaded into a much larger volume corresponding to an area (0.0006 m^2) over unit length at the same concentration, resulting in an amount of drug simulant per unit area and unit length of 0.6 mol. The higher amount of drug simulant per unit area coupled with the larger overall area of the domain of Case 3 is responsible for the lower final concentrations throughout the domain.

This analysis could also be applied to Case 1, where the initial concentration of drug simulant is focused along a boundary. The assumptions for Case 1 require the concentration of the drug simulant along that boundary to remain constant, providing a limitless supply of drug simulant into the wound domain of Case 1 until equilibrium is reached. This high concentration (with limitless supply) along the boundary of the domain in Case 1 creates and helps maintain a relatively large concentration gradient, which results in the fast rate of diffusion of drug simulant from the boundary into the wound domain of Case 1. This in turn produces the sharp slope of the transient concentration profile and the short time required for equilibrium to be reached within the wound domain (Figure 7). Similarly, the decreasing rate of diffusion in Case 2 and Case 3 relative to Case 1 can be explained by the amount of drug simulant and the location for the initial concentration of the drug simulant within the model.

Analysis of the most simplistic case of a drug simulant diffusing through a fixed concentration boundary and into a wounded dermal tissue domain, while perhaps not the most physiologically relevant case, has revealed that both the COMSOL simulation and analytical solution methodologies provide consistent results, provided that the simulation parameters reflect the mathematics that would be used to describe the physical conditions. In other words, while the models reflected herein are limiting cases of the potential models that might be produced resulting from the development of novel drug-delivering suture designs, one might extend the models here to reflect more physiologically relevant conditions. These conditions might include modifications to the sizes and properties of the domains, added phenomena such as a reaction to predict the reaction of a specific drug once delivery has occurred, or degradation of the suture domain such as when diffusive delivery occurs along with hydrolysis, as is the case with resorbable sutures.

As bioresorbable sutures have grown in popularity and polymeric biomaterials such as polyglycolic acid (PGA) have been employed in the development of sutures, coatings have been developed to reduce the risk of infection associated with sutures [35]—[37]

and reduce the tissue drag that results when placing a braided, multifilament suture [36], [37]. Experimental studies have been completed to determine the release rate of such antimicrobial substances while ensuring the sutures lose no structural stability due to the coatings [35]—[37]. Additionally, modeling [38], [39] and experimental [40]—[42] work has been completed to understand the mechanism by which a resorbable device will degrade and release therapeutics. With the development of polymeric biomaterials, interest has landed on resorbable sutures as a method of controlled drug delivery. Many of the efforts to investigate drug-release from resorbable sutures are experimental. Noorsal *et al.* designed an experimental study for the drug release of polyglycolide-*co*-trimethylene carbonate (Maxon) sutures, a bioresorbable suture, to determine the drug-release mechanism of the suture that degrades by hydrolysis [43]. In that study, the drug-release mechanism was concluded to be initially controlled by diffusion but later controlled by the polymer erosion during the suture's degradation.

Though as indicated above there have been multiple experimental (and some modeling) attempts for other bioresorbable drug delivery devices, few have explored the advantages of mathematically modeling (or examining via simulation) drug-delivering sutures. Casalini *et al.* are an exception to this as they looked at the drug-release of lidocaine from a bioresorbable suture placed in tissue and considered the kinetics that would occur during drug delivery to a living tissue [44]. Their drug release profile of lidocaine in a water and tissue environment resembles the trend shown in the concentration profiles developed with respect to time reported herein (Figures 7 and 12).

Further, few attempts have been documented throughout the literature that examine how drug release from a suture or other delivery device might decrease the occurrence of keloids. Many have indicated surgical excision as a treatment method of keloid scars once they arise [7], [8], [10], [14], [45], however, Berman and Bieley indicate that surgical methods of managing keloid scars can cause a recurrence rate of 45-100% in the patients that are treated [46]. They further state that surgical treatment of keloid scars can be combined with intradermal delivery of corticosteroids to reduce this recurrence rate to less than 50% [46], reiterating the importance of the work completed here. Though the work presented herein includes simulation results and only an analytical solution of the most simplistic case, intuition as well as the likeness to the drug-release profiles shown by others gives reason to believe that the COMSOL models developed for the purposes herein could be used to validate their results and therefore could be extended to more complicated physics. Such physics, as indicated earlier, could include consideration of the suture material as it has been shown that certain suture materials could promote the occurrence of keloids and other complications with scarring [47], [48]. When combined with analytical and experimental techniques, the ability to predict what might occur in these more complex physics and phenomena could increase the pace of discovery of new drug delivery devices, such as sutures, to improve wound healing.

Conclusions

Mathematical modeling and computer simulations often present a more viable option than experimentation for testing trial-and-error designs for new products such as biomedical devices or sutures. When used complementary to one another, an analytical approach can yield insight for the physics and associated conditions that can then be used to construct a simulation domain. This work considers three designs and associated simulation results for drug-delivering sutures, and the most simplistic design includes a complementary view of the analytical and simulation results for diffusion of a drug within a wound domain While the work presented herein accounts for only diffusion of a drug from a suture to the wound area, the nature of simulation lends itself to the adaptation towards understanding more complicated methods of drug delivery from sutures and other transdermal applications.

References

1. Guo, S. and DiPietro, L. Factors affecting wound healing. *J Den Res*, **89**, 219-229 (2010)

2. Mathieu, D. *Handbook on hyperbaric medicine*. Springer, New York, (2006)

3. Jorgensen, S. and Sanders, J. Mathematical models of wound healing and closure: A comprehensive review. *Med Biol Eng Comput*, **54**, 1297-1316 (2016)

4. Tam, J., Lau, K., Liu, C., To, M., Kwok, H., Lai, K., Lau, C., Ko, C., Leung, P., Fung, K., and Lau, C. The *in vivo* and *in vitro* diabetic wound healing effects of a 2-herb formula and its mechanisms of action. *J Ethnopharmacol*, **134**, 831-838 (2011)

5. Menke, N., Ward, K., Witten, T., Bonchev, D., and Diegelmann, R. Impaired wound healing. *Clin Dermatol*, **25**, 19-25 (2007)

6. [Dataset] Rui, P., Kang, K., and Albert, M. (2013) *National Hospital Ambulatory Medical Care Survey: 2013 Emergency Department Summary Tables*. Available from: http://www.cdc.gov/nchs/data/ahcd/nhamcs_emergency/2013_ed_web_tables.pdf

7. Bayat, A., McGrouther, D., and Ferguson, M. Skin scarring. *Br Med J*, **326**, 88-92 (2003)

8. Arno, A., Gauglitz, G., Barret, J., and Jeschke, M. Up-to-date approach to manage keloids and hypertrophic scars: A useful guide. *Burns*, **40**, 1255-1266 (2014)

9. Garg, S., Dahiya, N., and Gupta, S. Surgical scar revision: An overview. *J Cutan Aesthet Surg*, **7**, 3-1322 (2014)

10. Slemp, A. and Kirschner, R. Keloids and scars: A review of keloids and scars, their pathogenesis, risk factors, and management. *Curr Opin Pediatr*, **18**, 396-402 (2006)

11. Peacock, E. Control of wound healing and scar formation in surgical patients. *Arch Surg*, **116**, 1325-1329 (1981)

12. Uitto, J., Olsen, D., and Fazio, M. Extracellular matrix of the skin: 50 years of progress. *J Investig Dermatol*, **92**, 61S-77S (1989)

13. Granstein, R., Rook, A., Flotte, T., Hass, A., Gallo, R., Jaffe, H., and Amento, E. A controlled trial of intralesional recombinant interferon-γ in the treatment of keloidal scarring. *Arch Dermatol*, **126**, 1295-1302 (1990)

14. Kelly, A. Update on the management of keloids. *Semin Cutan Med Surg*, **28**, 71-76 (2009)

15. Asilian, A., Darougheh, A., and Shariati, F. New combination of triamcinolone, 5-fluorouracil, and pulsed-dye laser for treatment of keloid and hypertrophic scars. *Dermatol Surg*, **32**, 907-915 (2006)

16. Fitzpatrick, R. Treatment of inflamed hypertrophic scars using intralesional 5-FU. *Dermatol Surg*, **25**, 224-232 (1999)

17. Gupta, S. and Kalra, A. Efficacy and safety of intralesional 5-fluorouracil in the treatment of keloids. *Dermatol*, **204**, 130-132 (2002)

18. Kontochristopoulos, G., Stefanaki, C., Panagiotopoulos, A., Stefanaki, K., Argyrakos, T., Petridis, A., and Katsambas, A. Intralesional 5-fluorouracil in the treatement of keloids: an open clinical and histopathologic study. *J Am Acad Dermatol*, **52**, 474-479 (2005)

19. Nanda, S. and Reddy, B. Intralesional 5-fluorouracil as a treatment modality of keloids. *Dermatol Surg*, **30**, 54-57 (2004)

20. Blumenkranz, M., Ophir, A., Claflin, A., and Hajek, A. Fluorouracil for the treatment of massive periretinal proliferation. *Am J Opthalmology*, **94**, 458-467 (1982)

21. Dooley, S., Said, H., Gressner, A., Floege, J., En-Nia, A., and Mertens, P. Y-box protein-1 is the crucial mediator of antifibrotic interferon-γ effects. *J Biol Chem*, **281**, 1784-1795 (2006)

22. Hasegawa, T., Nakao, A., Sumiyoshi, K., Tsuboi, R., and Ogawa, H. IFN-γ fails to antagonize fibrotic effect of TGF-β on keloid-derived dermal fibroblasts. *J Dermatol Sci*, **32**, 19-24 (2003)

23. Larrabee, W., East, C., Jaffe, H., Stephenson, C., and Peterson, K. Intralesional interferon gamma treatment for keloids and hypertrophic scars. *Arch Otolaryngol Head Neck Surg*, **116**, 1159-1162 (1990)

24. Berman, B. and Kaufman, J. Pilot study of the effect of postoperative imiquimod 5% cream on the recurrence rate of excised keloids. *J Am Acad Dermatol*, **47**, S209-S211 (2002)

25. Berman, B., Harrison-Balestra, C., Perez, O., Viera, M., Villa, A., Zell, D., and Ramirez, C. Treatment of keloid scars post-shave excision with imiquimod 5% cream: A prospective, double-blind, placebo-controlled pilot study. *J Drugs Dermatol: JDD*, **8**, 455-458 (2009)

26. Van den Helder, C. and Hage, J. Sense and nonsense of scar creams and gels. *Aesthet Plast Surg*, **18**, 307-313 (1994)

27. Beck, L., DeGuzman, L., Lee, W., Xu, Y., Siegel, M., and Amento, E. One systemic administration of transforming growth factor-beta 1 reverses age-or glucocorticoid-impaired wound healing. *J Clin Investig*, **92**, 2841 (1993)

28. Brown, G., Curtsinger, L., Jurkiewicz, M., Nahai, F., and Schultz, G. Stimulation of healing of chronic wounds by epidermal growth factor. *Plast Reconstr Surg*, **88**, 189-194 (1991)

29. Knighton, D., Fiegel, V., Austin, L., Ciresi, K., and Butler, E. Classification and treatment of chronic nonhealing wounds: Successful treatment with autologous platelet-derived wound healing factors (PDWHF). *Ann Surg*, **204**, 322-329 (1986)

30. Shah, M., Foreman, D., and Ferguson, M. Control of scarring in adult wounds by neutralizing antibody

to transforming growth factor β. *Lancet*, **339**, 213-214 (1992)

31. Orgill, D. and Demling, R. Current concepts and approaches to wound healing. *Crit Care Medicine*, **16**, 899-908 (1988)

32. Edlich, R., Panek, P., Rodeheaver, G., Turnbull, V., Kurtz, L., and Edgerton, M. Physical and chemical configuration of sutures in the development of surgical infection. *Ann Surg*, **177**, 679-687 (1973)

33. Katz, S., Izhar, M., and Mirelman, D. Bacterial adherence to surgical sutures. *Ann Surg*, **194**, 35-41 (1981)

34. Edmiston, C., Seabrook, G., Goheen, M., Krepel, C., Johnson, C., Lewis, B., Brown, K., and Towne, J. Bacterial adherence to surgical sutures: Can antibacterial-coated sutures reduce the risk of microbial contamination? *J Am Coll Surg*, **203**, 481-489 (2006)

35. Gupta, B., Anjum, N., Gulrez, S., and Singh, H. Development of antimicrobial polypropylene sutures by graft copolymerization. II. Evaluation of physical properties, drug release, and antimicrobial activity. J *Appli Polym Sci*, **103**, 3534-3538 (2007)

36. Zurita, R., Puiggalu, J., and Rodriguez-Galan, A. Loading and release of ibuprofen in multi- and monofilament surgical sutures. *Macromol Biosci*, **6**, 767-775 (2006a)

37. Zurita, R., Puiggalu, J., and Rodriguez-Galan, A. Triclosan release from coated polyglycolide threads. *Macromol Biosci*, **6**, 58-69 (2006b)

38. Arosio, P., Busini, V., Perale, G., Moscatelli, D., and Masi, M. A new model of resorbable device degradation and drug release-Part I: Zero order model. *Polym Int*, **57**, 912-920 (2008)

39. Manca, D. and Rovaglio, M. Modeling the controlled release of microencapsulated drugs: theory and experimental validation. *Chem Eng Sci*, **58**, 1337-1351 (2003)

40. Crow, B., Borneman, A., Hawkins, D., Smith, G., and Nelson, K. Evaluation of *in vitro* drug release, pH change, and molecular weight degradation of (poly(L-lactic acid) and Poly(D,L-lactide-co-glycolide) fibers. *Tissue Eng*, **11**, 1077-1084 (2005)

41. Frank, A., Rath, S., and Venkatraman, S. Controlled release from bioerodible polymers: effect of drug type and polymer composition. *J Control Release*, **102**, 333-344 (2005)

42. Siegel, S., Kahn, J., Metzger, K., Winey, K., Werner, K., and Dan, N. Effect of drug type on the degradation rate of PLGA matrices. *European J Pharm Biopharm*, **64**, 287-293 (2006)

43. Noorsal, K., Mantle, M., Gladden, L., and Cameron, R. Degradation and drug-release studies of a poly(glycolide-co-trimethylene carbonate) copolymer (Maxon). *J Appl Polym Sci*, **95**, 475-486 (2005)

44. Casalini, T., Masi, M., and Perale, G. Drug eluting sutures: A model for *in vivo* estimations. *Int J Pharm*, **429**, 148-157 (2012)

45. Cosman, B., Crikelair, G., Ju, D., Gaulin, J., and Lattes, R. The surgical treatment of keloids. *Plast Reconstr Surg*, **27**, 335-358 (1961)

46. Berman, B. and Bieley, H. Adjunct therapies to surgical management of keloids. *Dermatol Surg*, **22**, 126-130 (1996)

47. Hohenleutner, U., Egner, N., Hohenleutner, S., and Landthaler, M. Intradermal buried vertical mattress suture as sole skin closure: Evaluation of 149 cases. *Acta Dermatovenerol Stockholm*, **80**, 344-347 (2000)

48. Niessen, F., Spauwen, P., and Kon, M. The role of suture material in hypertrophic scar formation: Monocryl vs. Vicryl-rapide. *Ann Plast Surg*, **39**, 254-260 (1997)

Acknowledgements

This work was funded by the Tennessee Technological University Department of Chemical Engineering and Office of Research and Economic Development. A special thanks goes to Dr. Yung-Way Liu for his assistance in development of mathematical concepts and solutions related to this work.

Appendix

Table 1. Parameters used in COMSOL simulations for each domain construction.

	Model #1: *Suture Utilizing a Fixed Concentration Boundary (Case 1)*	Model #2: *Drug-coated Solid Suture with Flux Boundary (Case 2)*	Model #3: *Drug-loaded Hollow Suture with Porous Wall and Flux Boundary (Case 3)*
Width of Interior Suture Domain	N/A	N/A	$2 * 10^{-4}$ m
Width of Porous Drug Coating or Porous Wall of Suture Domain	N/A	$8 * 10^{-5}$ m	$8 * 10^{-5}$ m
Width of Wounded Dermal Tissue Domain	$4.2* 10^{-4}$ m	$4.2 * 10^{-4}$ m	$4.2 * 10^{-4}$ m
Height of Domain(s)	$3 * 10^{-3}$ m	$3 * 10^{-3}$ m	$3 * 10^{-3}$ m
Study used in Interior Suture Domain	N/A	N/A	Time-dependent transport of diluted species
Study used in Porous Drug Coating or Porous Wall of Suture Domain	N/A	Time-dependent species transport in porous media (porosity = 0.3, 0.6, or 0.9)	Time-dependent species transport in porous media (porosity = 0.3, 0.6, or 0.9)
Study used in Wounded Dermal Tissue Domain	Time-dependent transport of diluted species	Time-dependent species transport in porous media (porosity = 1)[a]	Time-dependent species transport in porous media (porosity = 1)
Diffusion Coefficient of Drug Simulant	$1 * 10^{-10}$ m^2/s	$1 * 10^{-10}$ m^2/s	$1 * 10^{-10}$ m^2/s
Permeability	N/A	$1*10^{-6}$ m^2/s	$1*10^{-6}$ m^2/s
Partition Coefficient	N/A	1	1
Initial Concentration of Drug Simulant: Value (Placement)	1,000 mol/m^3 (Left Boundary)	1,000 mol/m^3 (Drug-Coated Portion of Suture Domain)	1,000 mol/m^3 (Interior Suture Domain)
Initial Concentration of Drug Simulant within Other Simulation Domain(s)	0 mol/m^3	0 mol/m^3	0 mol/m^3

[a]The time-dependent species transport in porous media study where the porosity is a value of one which replicates the time-dependent transport of diluted species study for Case 1.